WHITE PAPER

The Dynamic Simulation and Analysis of a Cycloidal Speed Reducer

Sandeep Thube & Todd Bobak

Sumitomo Drive Technologies

Sumitomo Machinery Corporation of America

Contents

Abstract

In industry, digital prototyping has become a valuable tool for the design and subsequent analysis of components for a proposed design. Prior to its maturation as a design tool, it was common to go through repeated physical iterations of a given design to assess form, fit and function. Investments in design time, prototype procurement and subsequent testing yielded long term product incubation periods from initial concept to final production. Current design modeling software allows for part design, unit assembly, loading and dynamic simulation of a component electronically – all without the procurement of a physical prototype. The results from such dynamic simulation can then be analyzed through finite element analysis to assess component functionality in its intended operational environment with an eye towards design optimization.

From the perspective of gear design, digital prototyping certainly affords the same advantages as has been described. Indeed, it is common to find electronic examples of 3D gearset with motion and loading condition imposed on them. It is less common, however, to find similar dynamic examples of the operation of a cycloidal type speed reducer where the kinematics of the reduction mechanism is completely different from that of the traditional involute gearing. This paper will explore a method of dynamically simulating a cycloidal type speed reducer where the generated internal loads will be used to assess the stresses acting on the one of the major reduction components contained within – namely, the cycloid disc.

Introduction

As the name implies, a speed reducer is a mechanical device whose function is to decrease the speed of a prime mover (i.e.: electric motor) while increasing the torque produced by the same prime mover. This increase in torque is directly proportional to the decrease in speed achieved through the speed reducer. Since the invention of rotating machines, the most common (and near exclusive) method of achieving this reduction of rotational speed has been through the interaction of gears in mesh with one another. Typically, the profile of a gear tooth follows an involute form (see Figure 1) and, over the course of years, techniques have been optimized to consistently reproduce this involute form during the manufacturing process.

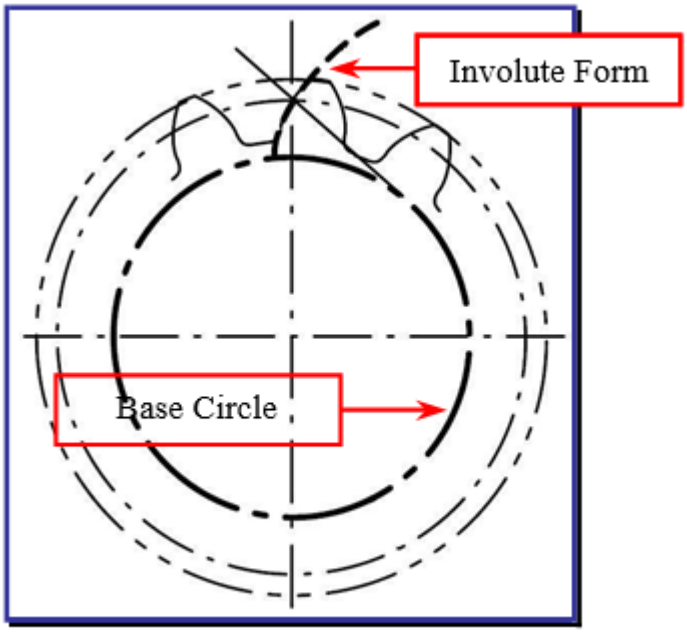

FIGURE 1: INVOLUTE TOOTH FORM

Despite this optimization, pitfalls remain in such traditional gearing. As an example, when in mesh, only a few of the teeth of one gear are actually engaged with those of the mating gear at any given time. Because of this, overloads (even if momentary in nature) may break one or more of the teeth on these gears. Additionally, in order to achieve higher reduction ratios, multiple gears may need to be incorporated into a single reducer thereby making it physically large in comparison to the amount of torque that it is able to deliver. Enter the Cycloidal type of speed reducer. The cycloidal reducer is a completely unique type of unique features will be verified by simulating part movements through dynamic analysis and observing/analyzing forces in the finite element analysis environment using dedicated 3D modeling software.

Features and Benefits

Since their inception in the 1930's, cycloidal type speed reducers have been successfully incorporated into a multitude of power transmission applications. Given the robust nature of the product, it is not uncommon to find examples that have successfully been in operation for periods of up to 25 years!

To understand how to model the mechanism digitally, one first needs to understand the basic components of a cycloidal gearbox and how they interact with each other. In referencing Figure 2 it can be seen that the speed reduction is achieved through the interaction of only three separate moving parts (the high speed shaft assembly, the cycloid discs and the slow speed shaft assembly):

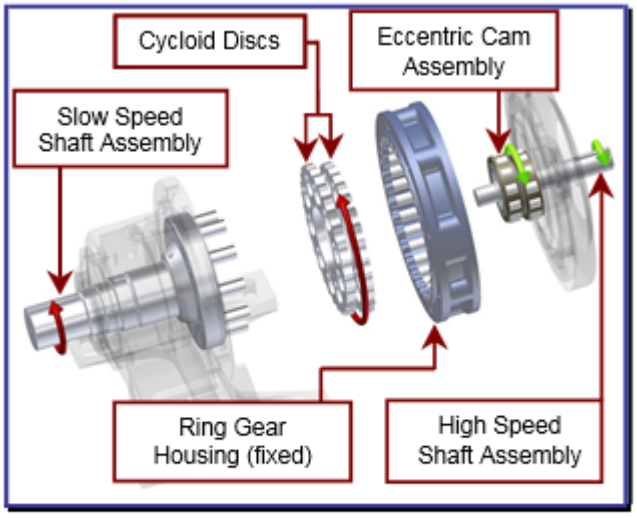

FIGURE 2: COMPONENTS OF A CYCLOIDAL SPEED REDUCER

The eccentric cam is pressed onto the high-speed shaft to complete the sub-assembly and, as it rotates, it rolls the Cycloid Discs around the inner circumference of the Ring Gear Housing. With this rotation of the cycloid discs, there occurs two points of contact with other reduction components of the assembly. First, there is a sliding motion of the external surface of the disc(s) against the rollers of the (fixed) Ring Gear Housing and second, there is a rotational motion of the disc(s) interacting with the Rollers of the Slow Speed Shaft. The Cycloidal Discs themselves rotate in a direction opposite that of the High Speed shaft and, while doing so, the lobes on outer edge of the discs progressively engage with the rollers attached to the inner perimeter of the Ring Gear Housing. This interaction produces a reversed rotation at a reduced speed. For each complete revolution of the high-speed shaft, the cycloid disc rotates one cycloidal tooth length in the opposite direction. Typically there is one less cycloidal tooth around the disc than there are pins in the fixed ring gear housing. This results in actual reduction ratios equal to the number of cycloidal teeth on the disc.

The reduced rotation of the cycloid discs is transmitted to the slow speed shaft via drive pins and rollers that engage with holes contained within the discs. Overall, this provides for greater torque transmission capability and offers an exceptionally smooth, vibration-free drive.

As may be seen in Figure 2, it is common for such systems to incorporate two discs and a double eccentric cam. For smaller unit sizes with corresponding smaller torque capacities, a single disc system driven by a single eccentric cam can be utilized.

Perhaps one of the greatest advantages of this cycloidal system over its involute gearing cousin is its shock load capability. With involute gearing, only a few number of teeth of one gear are engaged with those of the mating gear at any one time. As is seen in Figure 3, a shock load, even if it is short in duration, can lead to catastrophic tooth failure given the sharp radius of the tooth root (high stress concentration).

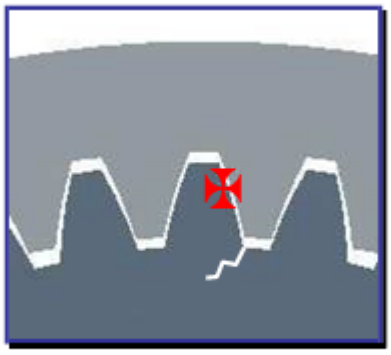

FIGURE 3: SHOCK LOADING IN INVOLUTE GEARING

With a cycloidal system, on the other hand, several of the lobes of the cycloidal discs are engaged with pins/rollers contained within the ring gear housing at any given time (FIGURE 4). This allows for greater load distribution among the reduction components that, in-turn, translates into greater shock load capacity.

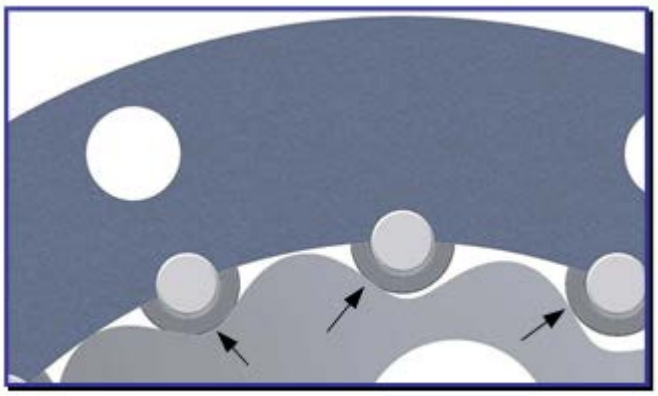

FIGURE 4: LOAD SHARING IN CYCLOIDAL MECHANISM

Given the relatively few number of reduction components that go into each cycloidal gearbox, an additional advantage of such mechanisms is that they are highly torque dense in comparison to gearboxes of similar capacities incorporating involute gearing.

Operating Principals

As noted previously, a Cycloidal speed reducer is fundamentally different from other speed reducers which incorporate traditional involute gearing as their reduction mechanism.

As may be seen in Figure 5, this Cycloidal technology cleverly combines the following two mechanisms into one:

1. A planet gear rotating about a fixed sun gear. For the Cycloidal reducer, the planet gear (P) has cycloidal-shaped teeth and the sun gear (S) has teeth in the style of circular pins. With this, the number of teeth in the planet gear is one or two less than that of the sun gear.
2. A constant speed internal gearing mechanism.

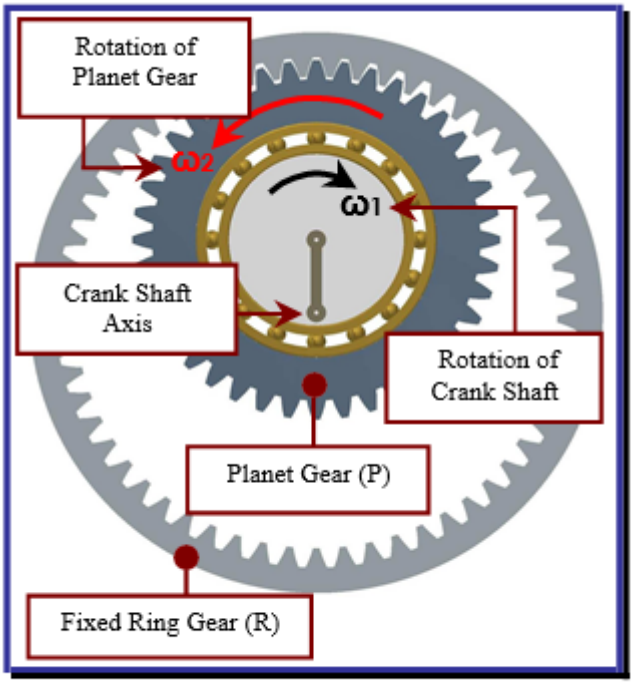

FIGURE 5: PRINCIPLE OF INTERNAL PLANETARY GEARING

The velocity ratio between the rotating Crank Shaft and the rotating Planet Gear is mathematically defined as:

$$\frac{\omega_2}{\omega_1} = 1 - \frac{R}{P} = -\frac{R-P}{P} \qquad \text{(Equation i)}$$

Where:

P = the number of teeth in the planet gear
R = the number of teeth in the ring gear
ω1= the angular velocity of the crankshaft about the sun gear
ω2= The angular velocity of the planet gear about its own axis

With the number of teeth in the ring gear greater than those in the planet gear by a value of 1 or 2, the velocity ratio as described by equation 1 is always maximized. Specifically, if R – P = 1, then Equation 1 can be re-written as:

$$\frac{\omega_2}{\omega_1} = -\frac{1}{P} \qquad \text{(Equation ii)}$$

Likewise, if R – P = 2, the velocity ratio defined by Equation 1 then becomes:

$$\frac{\omega_2}{\omega_1} = -\frac{2}{P} \qquad \text{(Equation iii)}$$

Given Equations ii and iii, it can be said that, as the crank shaft rotates at the angular velocity of ω1 about the axis of the ring gear, the angular velocity of the planet gear can be mathematically

established as:

$$\omega_2 = -\frac{\omega_1}{P} \text{ or } \omega_2 = -\frac{2\omega_1}{P} \quad \text{(Equation iv)}$$

In Equation iv it is important to note that the negative sign indicates that the planet gear is rotating in a direction opposite that of the sun gear.

Figure 6 represents a cycloidal type speed reducer where the circular teeth (pins) represent the ring gear and the epitrochoid-curved teeth replace the planet gear.

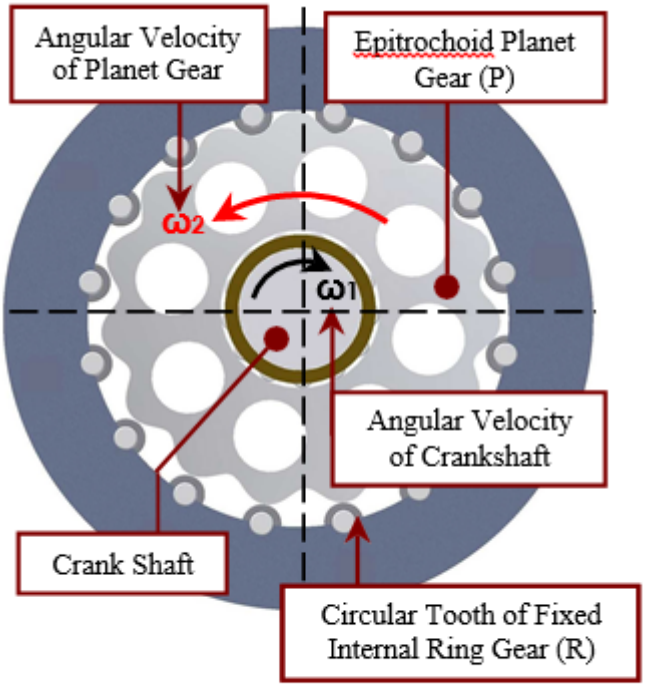

FIGURE 6: EPITROCHOID PLANET GEAR - CIRCULAR (PIN) TOOTH SUN GEAR COMBINATION

Referencing Figure 7, it can be then seen that the rotation of the planet gear about its own axis is taken out through a constant speed internal gearing mechanism:

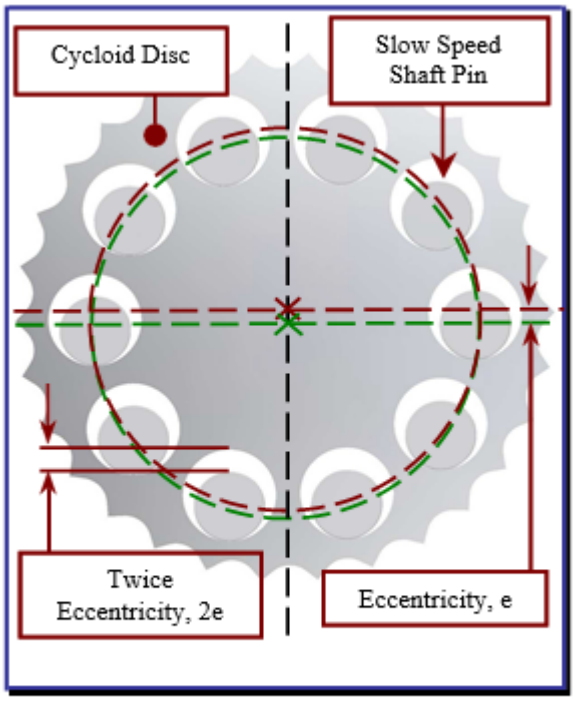

FIGURE 7: CONSTANT SPEED INTERNAL GEARING

Finally, in Figure 8, the pins of the slow speed shaft are evenly spaced on a circle that is concentric to the axis of the sun gear. These pins transmit the rotation of the planet gear by rolling internally on the circumference of the bores of each planet gear (or cycloid disc):

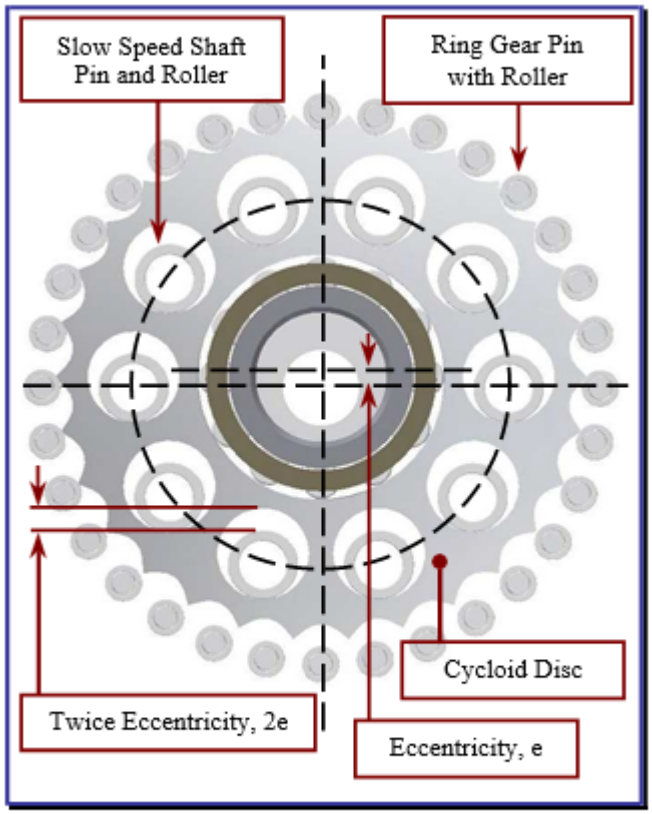

FIGURE 8: COMBINATION OF PLANET/SUN GEAR AND CONSTANT SPEED INTERNAL GEAR

The diameter of the bores minus the diameter of the slow speed shaft pins is equal to twice the eccentricity value of the crank shaft (eccentric). As a result, this mechanism smoothly transmits only the rotation of the planet gear around its own axis to the slow speed shaft.

Dynamic Simulation

Dynamic simulation is used prior to the FEA analysis to investigate the time instance at which the cycloidal disc experiences the highest load in an operating cycle. Dynamic simulation helps to analyze a combined effect of relative motions of moving parts, input parameters and external loads on the mechanism with respect to time.

In selecting a model to apply the dynamic simulation routine to, primary attention was given to efficiently optimizing the simulation time. Given this, a cycloidal system incorporating one disc (verses two) was selected to model. Likewise, a unit reduction ratio of 15:1 was chosen for the model.

Establishing relative motions amongst interacting parts of the gearbox assembly is an important step in simulation building process. Current software facilitates such dynamic motions by creating “joints” between two parts in an assembly to define a mechanism. These joints allow us to add degrees of freedoms for components, which initially are considered immovable in the simulation environment. For instance, a revolution joint authorizes an angular degree of freedom while creating relationship between cylindrical faces and cylindrical axes of two components. In our assembly, this joint is applied at several places; one of them is between eccentric bearing and cycloidal disc as shown in Figure 9.

These two parts are constrained not to move in all directions, but allowed to rotate along Y-axis.

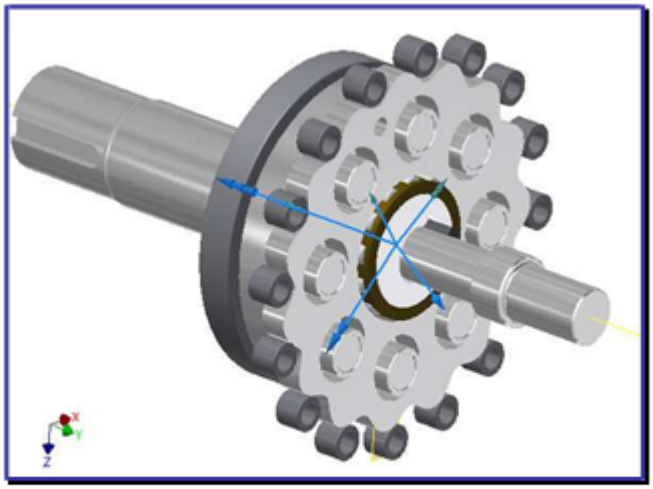

FIGURE 9: ARROWS SHOW LOCATION AND ORIENTATION OF THE JOINT ON ECCENTRIC BEARING AND CYCLOIDAL DISC.

3-D contact force joint is also used in the mechanism to establish a contact between the parts, like cycloidal disc and rollers of ring gear housing, that separate from each other in some time intervals. Table 1 details the joints applied to different components to form the mechanism.

TABLE 1: JOINTS OF SIMULATION MODEL

No.	Components	Joint Type	Qty
1	Input shaft/ ground	Revolution	1
2	Eccentric bearing/ Cycloidal disc	Revolution	1
3	Cycloidal disc/ Ring gear rollers	3-D contact	16
4	Ring gear pin/ Ring gear rollers	Revolution	16
5	Cycloidal disc/ LSS rollers	3-D contact	8
6	Low speed shaft pin/ LSS rollers	Revolution	8
7	Output shaft/ ground	Revolution	1

To further optimize dynamic simulation performance, certain components within the model of the speed reducer are eliminated from the simulation environment. These components include: casings, the ring gear housing, oil seals etc. The input shaft, eccentric bearing and balance weight are considered as one entity (welded group) to minimize the number of joints thereby minimizing the associated computer calculation time. Instances can occur where the number of assembly constraints in a model removes more degrees of freedom than the assembly itself contains. That is, the degrees of freedom minus the constraints of all components is less than zero. This is known as a redundancy. Although a redundant model shows correct relative movements in the animation, the reaction forces

obtained as an output may be incorrect. For the simulation described herein, the current model is checked and confirmed as a non- redundant mechanism.

Joints permit to define initial kinematic status of parts and establish imposed motions. Input shaft of the gearbox is set to 1750 rpm and 1,040 in•lbs load is applied on output shaft to simulate full load condition for the cycloidal speed reducer under consideration.

Simulation outputs are generated at joints. Depending upon the type of joint, parameters like position, velocity, acceleration, force and moments can be analyzed with varying time in the form of graphs. We set simulation time about 0.515 sec, and total numbers of steps are 172. In this period of time, the cycloidal disc completes 1 complete rotation within the ring gear housing. Based on simulation result, the average transmission ratio is 15.007:1, which is almost equal to the theoretical transmission ratio 15:1. The relation between input and output shaft rotational speed is shown in Graph 1. This proves the kinematic reliability of the simulation model.

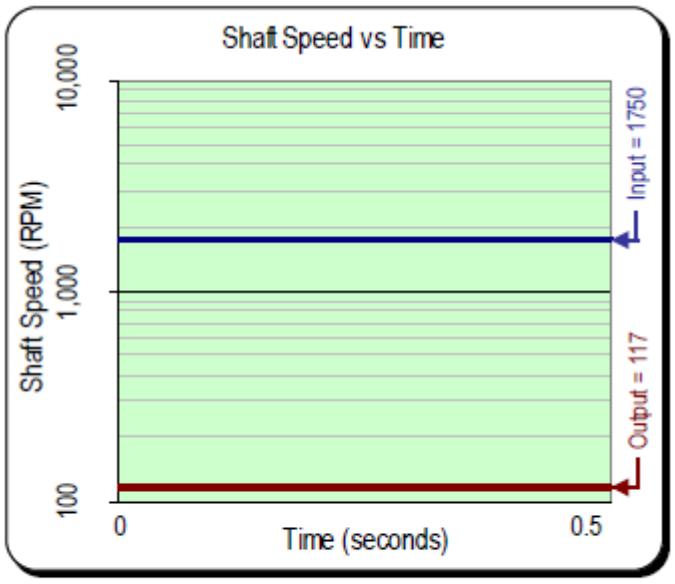

GRAPH 1: COMPARISON OF INPUT AND OUTPUT SPEEDS IN THE SIMULATION ENVIRONMENT

Torques of input and output shafts obtained from the simulation results, as shown in Graph 2, also confirms accuracy of the model. Output torque is almost 15 times that of the input torque (NOTE: operational efficiency losses were not incorporated into the model for the simulation)

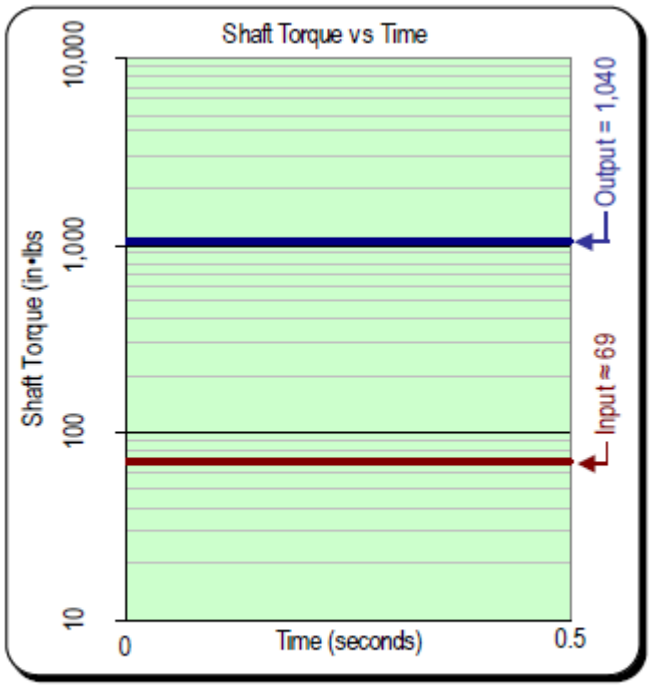

GRAPH 2: COMPARISON OF INPUT AND OUTPUT TORQUES IN THE SIMULATION ENVIRONMENT

Simulation Results

Of the many benefits obtained from conducting such a dynamic simulation on the cycloidal mechanism is the fact that the simulation is able to provide numeric values for the contact forces occurring between components interacting with each other within the mechanism. Post simulation, contact forces can be sorted for the highest magnitude in a given time period thereby giving an idea of the maximum load which is occurring during the time period under consideration. In turn, these contact forces can be incorporated onto a component of interest for subsequent analysis via the Finite Element Analysis method. In the case of the previously addressed simulation, a time of 0.417 seconds has been identified as a highly stressful moment for cycloidal disc. FEA analysis is performed on the disc at this time interval.

In the case of the cycloidal disc, three unique series of forces are acting on the disc at any moment of time. In referring Figure 10, it can be seen that these forces are incurred from:

1. The interaction of the disc with the rollers of the ring gear housing,
2. The interaction of the disc with the rollers of the slow speed shaft pins, and
3. The interaction of the eccentric cam with the large bore of the cycloid disc.

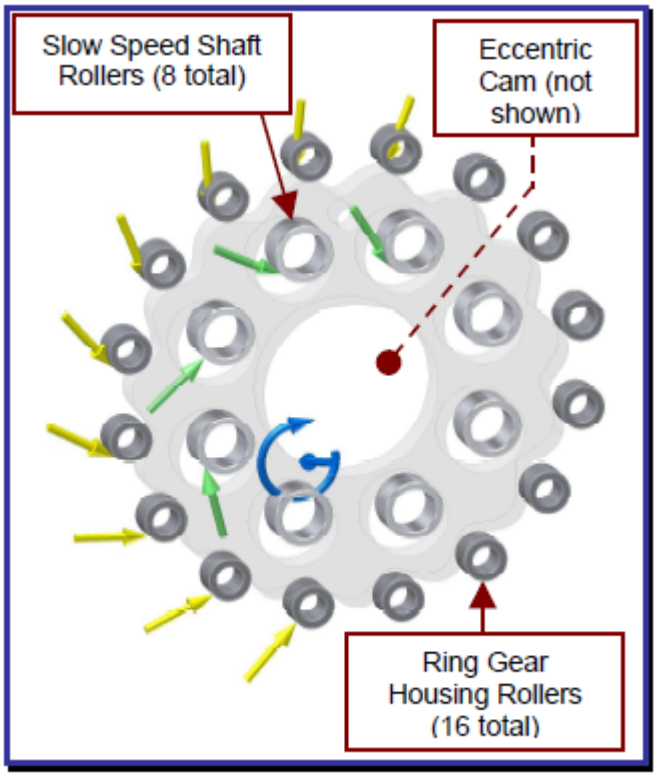

FIGURE 10: FORCES ACTING ON CYCLIODAL DISC

Again referencing Figure 10, it is interesting to note that, in this case, 9 of the 16 rollers of the ring gear housing (~ 55%) are sharing the induced load. From the perspective of the analysis itself, it is further important to note that while the use of straight arrows may imply the presence point loads on the Components themselves, the interaction of the rollers may imply the presence point loads on the components themselves, the interaction of the rollers (ring gear rollers, slow speed shaft rollers) on the cycloid disc assures that the loading is acting across the entire face of the contact surface. Figure 11 represents the results of the first iteration of the FEA process. This figure details the Von Mises stress acting on the Rollers and the Cycloid Disc:

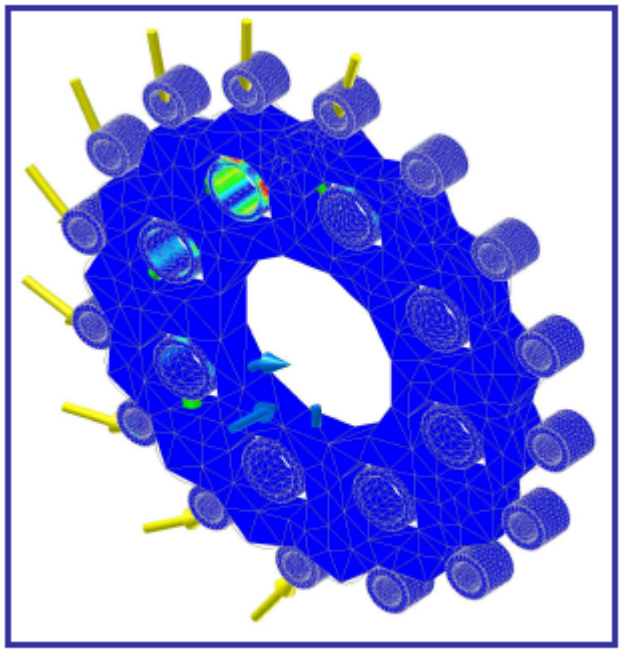

FIGURE 11: VON MISES STRESS ON ROLLERS AND CYCLOID DISC

As indicated by the presence of red in FIGURE 11 the maximum Von Mises stress is acting on one of the Slow Speed Shaft rollers at the particular moment in time that this simulation was run. This is not unusual considering that the greatest forces, at this moment in time, are those acting on that particular component.

With the area of highest stress identified within the assembly, the subsequent results can be refined by increasing the mesh density on the roller with the highest identified stress concentration. Additionally, the mesh density of the through-hole in which this roller interacts can also be increased for further result refinement. These mesh refinements can be clearly seen in FIGURE 12

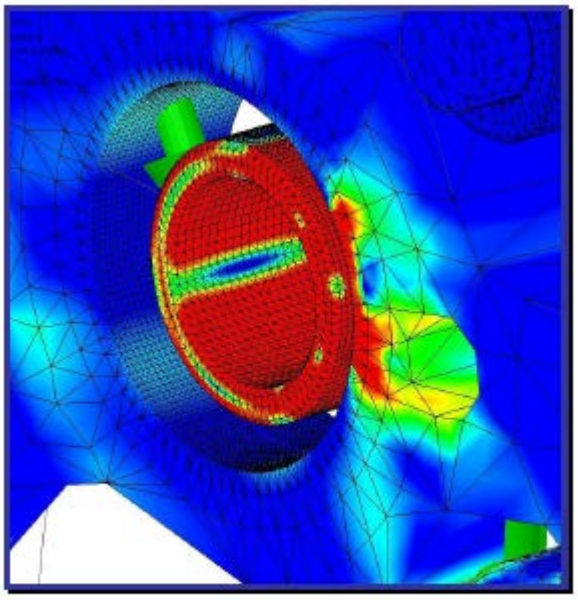

FIGURE 12: VON MISES STRESS AFTER INCREASE IN LOCAL MESH DENSITY

The mesh refinement is made to the point where the convergence results are less than 5%. Recalling that the part of interest for this particular case is the cycloid disc itself, Figure 13 shows this disc excluding the presence of the rollers. In essence, the figure details the Von Mises stress of the disc resulting from the loads specifically acting upon it:

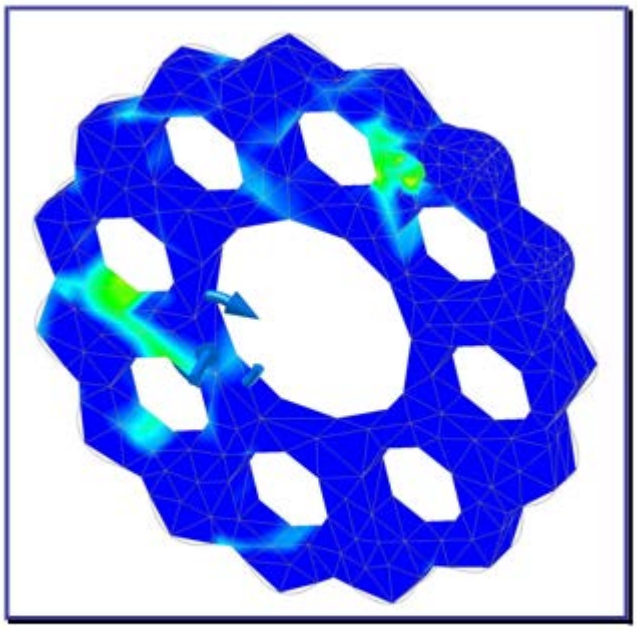

FIGURE 13: VON MISES STRESS ON CYCLOID DISC

At the moment of time considered, the maximum stress acting on the disc is occurring at the interface between the Slow Speed Shaft Rollers and the disc. In this regard it is important to note that the

stress is not concentrated around one of the through holes but rather is shared (not equally) with other through holes on the circle diameter. Likewise, a review of the lobes on the outer circumference of the disc indicates that, as expected, heightened stresses occur at the contact positions where the rollers of the ring gear housing interact with the disc surface (Figure 14)

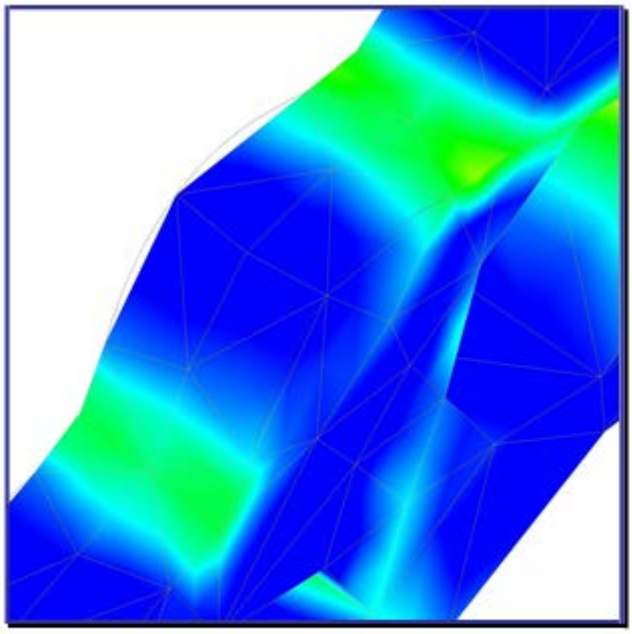

FIGURE 14: VON MISES STRESS ON DISC LOBES

interaction of the Slow Speed Shaft Rollers with the disc, the stresses arising from the interaction of the Ring Gear Rollers with the disc are distributed onto more than one lobe of the disc. A review of the associated stress values suggests that these stresses are not equally distributed onto the engaged lobes.

Conclusion

Given a clear understanding of the underlying operating principles, the dynamic simulation of the unique cycloidal speed reducer can be accurately achieved. The subsequent finite element analysis effectively served to clearly validate the shock load capability of the reduction mechanism.

References

Wasim, Y., 2009, *AutoDesk Inventor Simulation 2010*, Butterworth-Heinemann

Kurowski, P., 2004, *Finite Element Analysis for Design Engineers*, SAE International